# Quantitative Fundus Autofluorescence in Mice: Correlation With HPLC Quantitation of RPE Lipofuscin and Measurement of Retina Outer Nuclear Layer Thickness

Janet R. Sparrow,[1,2] Anna Blonska,[1] Erin Flynn,[1] Tobias Duncker,[1] Jonathan P. Greenberg,[1] Roberta Secondi,[1] Keiko Ueda,[1] and François C. Delori[3]

[1]Department of Ophthalmology, Columbia University, New York, New York
[2]Departments of Pathology and Cell Biology, Columbia University, New York, New York
[3]Harvard Medical School, Schepens Eye Research Institute, Boston, Massachusetts

Correspondence: Janet R. Sparrow, Department of Ophthalmology, Columbia University, 630 W. 168th Street, New York, NY 10032; jrs88@columbia.edu.

Submitted: December 13, 2012
Accepted: March 22, 2013

Citation: Sparrow JR, Blonska A, Flynn E, et al. Quantitative fundus autofluorescence in mice: correlation with HPLC quantitation of RPE lipofuscin and measurement of retina outer nuclear layer thickness. *Invest Ophthalmol Vis Sci*. 2013;54:2812–2820. DOI:10.1167/iovs.12-11490

**Purpose.** Our study was conducted to establish procedures and protocols for quantitative autofluorescence (qAF) measurements in mice, and to report changes in qAF, A2E bisretinoid concentration, and outer nuclear layer (ONL) thickness in mice of different genotypes and age.

**Methods.** Fundus autofluorescence (AF) images (55° lens, 488 nm excitation) were acquired in albino *Abca4*$^{-/-}$, *Abca4*$^{+/-}$, and *Abca4*$^{+/+}$ mice (ages 2–12 months) with a confocal scanning laser ophthalmoscope (cSLO). Gray levels (GLs) in each image were calibrated to an internal fluorescence reference. The bisretinoid A2E was measured by quantitative high performance liquid chromatography (HPLC). Histometric analysis of ONL thicknesses was performed.

**Results.** The Bland-Altman coefficient of repeatability (95% confidence interval) was ±18% for between-session qAF measurements. Mean qAF values increased with age (2–12 months) in all groups of mice. qAF was approximately 2-fold higher in *Abca4*$^{-/-}$ mice than in *Abca4*$^{+/+}$ mice and approximately 20% higher in heterozygous mice. HPLC measurements of the lipofuscin fluorophore A2E also revealed age-associated increases, and the fold difference between *Abca4*$^{-/-}$ and wild-type mice was more pronounced (approximately 3–4-fold) than measurable by qAF. Moreover, A2E levels declined after 8 months of age, a change not observed with qAF. The decline in A2E levels in the *Abca4*$^{-/-}$ mice corresponded to reduced photoreceptor cell viability as reflected in ONL thinning beginning at 8 months of age.

**Conclusions.** The qAF method enables measurement of in vivo lipofuscin and the detection of genotype and age-associated differences. The use of this approach has the potential to aid in understanding retinal disease processes and will facilitate preclinical studies.

Keywords: Abca4, RPE lipofuscin, quantitative fundus autofluorescence, mouse, bisretinoid

Fundus autofluorescence (AF) imaging using a confocal scanning laser ophthalmoscope (cSLO) is a noninvasive approach to monitoring the natural autofluorescence of the retina generated from the bisretinoids of lipofuscin in RPE. In early studies of fundus AF in human subjects, quantitation at discrete positions on the fundus was done by noninvasive spectrophotometry.[1–3] This work contributed to our understanding of the relationship between RPE lipofuscin accumulation and age, and demonstrated increases in fundus AF in retinal disorders, such as recessive Stargardt disease,[3,4] caused by mutations in the ATP-binding cassette (ABC) transporter *ABCA4*.[5] Conversely, imaging of fundus AF by cSLO records the spatial distribution of fundus AF[6–9] and is valuable as a means to monitor specific patterns of AF in human retinal diseases, including age related macular degeneration and RP.[9–11] Some studies have reported comparative assessment of fundus AF enabled by adherence to well-defined imaging protocols.[12,13]

Fundus AF imaging by cSLO also has aided the characterization of retina in animal models.[14–16] Several therapeutic strategies aimed at alleviating vision loss in recessive Stargardt disease have been tested preclinically in *Abca4*$^{-/-}$ and *Rdh8*$^{-/-}$ *Abca4*$^{-/-}$ mice. These approaches include vector-based gene therapies,[17,18] and the employment of compounds that limit the visual cycle.[19–23] In these preclinical trials, high performance liquid chromatography (HPLC) quantitation of A2E served as the primary therapeutic outcome measure. Since HPLC quantitation requires enucleation and extraction of tissues, longitudinal studies in the same mouse are not possible.

As an alternative measure, we have been working to develop quantitative fundus autofluorescence (qAF) imaging in the mouse. This work follows a recent study that introduced a robust method for quantifying fundus AF in human subjects.[24] This approach is based on the principle that fundus AF intensities can be measured objectively if normalized to a standard reference incorporated into the imaging device. The reference enables compensation for changes in laser power and detector gain.[24] Here, we have adopted the same approach to acquire standardized fundus AF measurements in mice using a Spectralis (Heidelberg Engineering, Heidelberg, Germany) instrument, modified by the addition of an internal fluorescent

reference, and by the incorporation of an aperture to reduce the laser beam diameter and detection pupil so that they can be accommodated by the smaller size of the mouse pupil. We also compared fundus AF measurements in the presence and absence of a contact lens used to retard cataract formation. We studied albino *Abca4*$^{-/-}$, *Abca4*$^{+/-}$, and *Abca4*$^{+/+}$ mice at different ages, and we compared qAF values with HPLC measurements of the RPE bisretinoid A2E.

## Methods

### Animals

Albino *Abca4/Abcr* null mutant mice (*Abca4*$^{-/-}$), *Abca4*$^{+/-}$ heterozygous mice, and *Abca4*$^{+/+}$ wild type mice, all of which were homozygous for Rpe65-Leu450, were reared and genotyped.[25] Albino *BALB/c* wild-type mice were obtained from The Jackson Laboratory (Bar Harbor, ME). All animals were housed according to standard 12-hour on-off cyclic lighting with in-cage illuminance of 30 to 80 lux. Mice of each *Abca4* genotype at ages 2, 4, 6, 8, and 12 months were used for imaging. After euthanization and enucleation, murine eyes were extracted for HPLC analysis or were processed for histology. The research was approved by the Institutional Animal Care and Use Committee (IACUC), and was performed in accordance with the ARVO Statement for the Use of Animals in Ophthalmic and Visual Research.

### Fundus AF Image Acquisition

Mice were anesthetized with an intraperitoneal injection of ketamine (100 mg/kg) and xylazine (10 mg/kg). The pupils were dilated to a diameter of approximately 2.5 mm (range 2.1–2.9) by instillation of 1% tropicamide and 2.5% phenylephrine (Akorn, Inc., Lake Forest, IL) 15 minutes before image acquisition. The pupil size was measured either by placing a ruler on the surface of the eye or with the ruler tool in Photoshop CS5 (Adobe, San Jose, CA) after acquiring an image of the pupil at +50 diopters (D), as described previously.[14]

Cataract formation due to corneal surface drying in anesthetized mice is known to occur.[26] Thus, as protection, a drop of lubricant GenTeal Liquid Gel (Novartis, East Hanover, NJ) was applied topically to the corneas of both eyes before image acquisition. In addition, a custom made contact lens (PMMA mouse lens, back optic zone radius of 1.7 mm, total diameter of 3.2 mm, center thickness of 0.4 mm, straight sides; Cantor and Nissel, Brackley, UK) was placed on the eye to be imaged or on the fellow eye (as indicated) to prevent corneal desiccation. The contact lens was centered carefully and we verified the absence of air bubbles. To avoid image artefacts, whiskers were trimmed carefully and excess gel was removed gently from the corneal surface. The mouse was positioned on a custom-made platform, and body temperature was maintained and monitored with a heating blanket interfaced with temperature controller (Model TC-1000) and thermistor probe (YSI-451; IITC Life Science, Woodland Hills, CA).

AF images (55°, 488 nm excitation) were acquired with a confocal scanning laser ophthalmoscope (Spectralis HRA; Heidelberg Engineering). With the 55° wide-field lens, the diameter of the incident laser beam at the mouse pupil (plane) is 1.7 mm, and the diameter of the detection pupil is 3.4 mm (the detection pupil is the area of the mouse pupil that collects light from the fundus). Since a mouse pupil dilates only to approximately 2 mm in diameter, with this configuration a significant portion of the fundus fluorescence would not be detected and a correction to account for variations in pupil diameter of the mouse would be required. To avoid these problems, the instrument was modified internally by the manufacturer such that the diameter of the incident laser beam and the diameter of the detection pupil were identical and equal to 0.98 mm. The choice of aperture was the result of experimentation with different aperture configurations. A larger common aperture provided more signal for the same laser power, but image quality was diminished and focusing required a shift to compensate for chromatic aberrations. Laser power was adjusted to approximately 280 μW. Sensitivity settings on the Spectralis were 95 to 100 (settings >100 may produce nonlinear effects).

The Spectralis was equipped additionally with an internal fluorescence reference[24] to account for fluctuations in laser power and detector sensitivity. The reference was mounted in the intermediate retinal plane of the camera, such that it was imaged simultaneously with the fundus and always was in focus.

Images were acquired under dim room light. In near infrared reflectance mode (NIR-R, 820 nm), the camera was positioned to ensure that the 55° field was centered on the optic disc and the fundus was illuminated evenly. The focus was adjusted to the point where the reflecting signal across the fundus was maximal. After switching to AF mode (488 nm), the retina was preexposed for 20 seconds to bleach visual pigment.[14,24] The detector sensitivity was adjusted to ensure sufficient signal strength within the linear range of the device. The focus was left unchanged. Nine successive frames then were acquired with the high-speed mode (8.9 images/s). The frames were aligned and averaged with the system software and saved in the "nonnormalized" mode (no histogram stretching) to generate the AF image for analysis. To assess repeatability in a group of *Abca4*$^{-/-}$ mice, two consecutive images were acquired in the first session without moving the camera or mouse. For the second session, mouse and camera were moved, and realigned, the camera settings were readjusted, and another set of images was recorded. The Spectralis was tested previously and described to be linear for exposures that produced GL < 175.[24]

### Image Analysis

All fundus AF images were analyzed using a dedicated image analysis program written in IGOR (WaveMetrics, Inc., Lake Oswego, OR). Mean gray levels (GL) were recorded from 8 predefined segments around the optic disc (Fig. 1). Blood vessels were excluded by histogram analysis as has been described previously.[24] To calculate qAF, the mean GLs of the reference ($GL_R$), of each segment on the fundus ($GL_F$), and of the zero light ($GL_0$, equivalent GL given by the software) were combined as $qAF = RCF \times (GL_F - GL_0)/(GL_R - GL_0)$. RCF is the reference calibration factor (0.7 in this study), which is obtained by calibration with an external master reference.[24] All qAF values reported in this study were calculated as the mean qAF of all 8 segments (Fig. 1). qAF values are based on means of at least 2 images obtained from the first eye recorded to minimize the likelihood that cataract formation would affect qAF results.

### Histometric Analysis

Following sacrifice and enucleation, eyes were immersed in 4% paraformaldehyde for 24 hours at 4°C. Sagittal paraffin serial sections of mouse retina were prepared, and stained with hematoxylin and eosin. The section positioned most centrally in the optic nerve head (ONH) was selected and imaged with the 20× objective using a digital imaging system (Leica

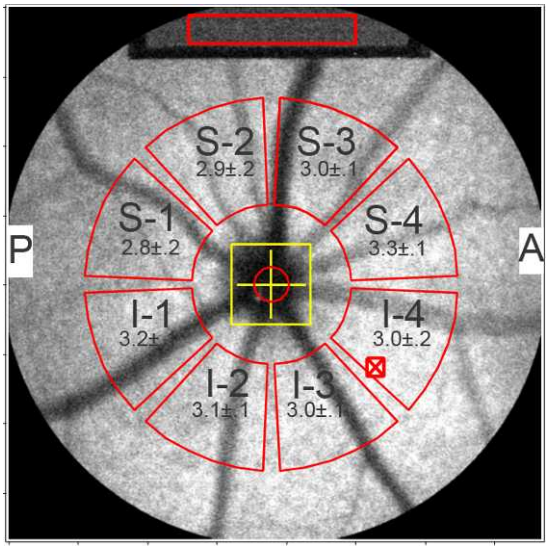


FIGURE 1. Quantitative fundus AF in the mouse. Fundus AF image of right eye of a *Abca4*$^{-/-}$ mouse (age 8 months). For quantitation, mean GLs are determined in 8 segment (outlined in *red*) located between 8.25° and 19.25° from the center of the *disc* (*yellow cross*). The GLs are normalized to values determined for the internal fluorescent reference (*Top*: sampling area is indicated by *red rectangle*). The reference always is in focus with the fundus image. Superior (S1–S4) and inferior (I1–I4) segments are labeled. A, anterior; P, posterior. The software minimized interference from blood vessels by analyzing the histogram of the GLs in each segment.[24] Values presented in each segment (*red*) are qAF ± SEM (right eyes of 8 mice).

Application suite; Leica Microsystems, Welzlar, Germany) and composite images were created in Photoshop CS5. Outer nuclear layer (ONL) thickness then was measured at 200 μm intervals superior and inferior to the edge of the ONH along the vertical meridian.[25] The measurements were made using the Photoshop CS5 ruler tool and a custom measurement scale. ONL width in pixels was converted to micrometers (1 pixel = 0.23 μm). For groups of *Abca4*$^{-/-}$, *Abca4*$^{+/-}$, and *Abca4*$^{+/+}$ mice at defined ages, mean ONL thickness at each position along the vertical meridian was plotted as a function of eccentricity from the ONH.

### Quantitative HPLC

Mouse eyecups were pooled (4–8 eyes per sample depending on genotype), homogenized, extracted, and filtered, and the solvent was evaporated as described previously.[27] The extract was redissolved in chloroform/methanol, and A2E and iso-A2E were measured by HPLC (Alliance system; Waters Corp., Milford, MA).[28] Absorbance peaks were identified by comparison with external standards. Molar quantities per eye were calculated from peak areas using standard concentrations determined spectrophotometrically together with published extinction coefficients. Values from each sample were calibrated to the number of eyes in a sample and were expressed as picomoles/eye. Mean ± SEM for each genotype and age were obtained by averaging multiple independent samples.

### Statistical Analyses

Analyses were performed using Prism 5 (GraphPad Software, La Jolla, CA) and the statistical tests as indicated.

## RESULTS

### Contact Lens and Cataract Formation

To assess the effect of contact lens absorption on qAF values, we imaged one eye of 4 mice (BALBc, age 10 months), first with a contact lens on (3 images) and immediately after with the contact lens removed (3 images, Fig. 2). qAF values were consistently lower (average difference 39%) in the presence of the contact lens and the qAF values also were more variable (mean ± SD with contact lens 0.97 ± 0.30, without contact lens 1.61 ± 0.11). The coefficient of variation was 31.3% in the case of the contact lens and 6.8% with no contact lens.

To evaluate cataract formation during imaging in the absence of a contact lens, we acquired images for 7 minutes in 30- to 60-second intervals (Figs. 3A, 3B). Without use of the contact lens, qAF values started decreasing 30 seconds after the initial image was acquired at time zero. After 90 seconds qAF had decreased by approximately 14% and after 300 seconds a 50% decline was observed (Fig. 3B). Conversely, in the presence of the contact lens, qAF values decreased only 1.8% over 300 seconds of serial imaging (Fig. 3A).

A correction factor, to account for the artificially low qAF values in the presence of a contact lens, was not achievable, since in our hands the extent of attenuation was not sufficiently constant. Consequently, AF images used for comparison of qAF among varying genotypes and age (discussed below) were acquired without a contact lens, and these images were acquired during a relatively short interval of 60 seconds. Meanwhile, the contact lens was placed on the fellow eye to protect the cornea and lens.

### Focusing

We evaluated the effect of focusing errors on qAF values (*Abca4*$^{-/-}$ mouse, age 10 months) using a contact lens to minimize a potential bias from cataract formation. The focus first was adjusted in NIR-R mode to the point where the reflectance signal across the fundus was the highest. This focus setting served as our reference point, as it corresponded to the focus that would have been chosen for AF imaging as part of our standard imaging protocol. Subsequently, in SW-AF mode, we varied the focus in intervals of 2 D in the hyperopic and myopic directions, and acquired 2 images at each focus setting. Calculation of mean qAF at each focus revealed that the focus chosen in NIR-R mode also exhibited the highest qAF values (Fig. 3C). Defocusing by +2 D decreased qAF values by 3.4%. A change of +4 and −4 D resulted in decreases of 10.2% and 5.8%, respectively. A hyperopic shift of +20 D caused a 45.3% decline in qAF and a myopic shift of −15 D caused a 22.8% decrease. The decrease in qAF was more rapid in the hyperopic direction. Foci used for AF imaging across all mice in our study ranged from −5.8 to + 30.4 D. Between sessions the focus only differed by 2 to 3 D. Thus, a focusing error would have contributed less than 10% to qAF variation.

### Spatial Distribution of qAF

We compared gray scale intensity levels in each of 8 sampling segments (Fig. 1) to determine whether AF intensity exhibited spatial differences across the mouse fundus. For *Abca4*$^{-/-}$ mice (8 months), the mean qAF ranged from 2.79 to 3.27 and for *Abca4*$^{+/+}$ mice (8 months) the range was 1.32 to 1.5 qAF units. By one-way ANOVA, differences in qAF values among the segments were not statistically significant in either the *Abca4*$^{-/-}$ ($P = 0.38$, $n = 8$) or *Abca4*$^{+/+}$ mice ($P = 0.82$, $n = 12$).

Investigative Ophthalmology & Visual Science

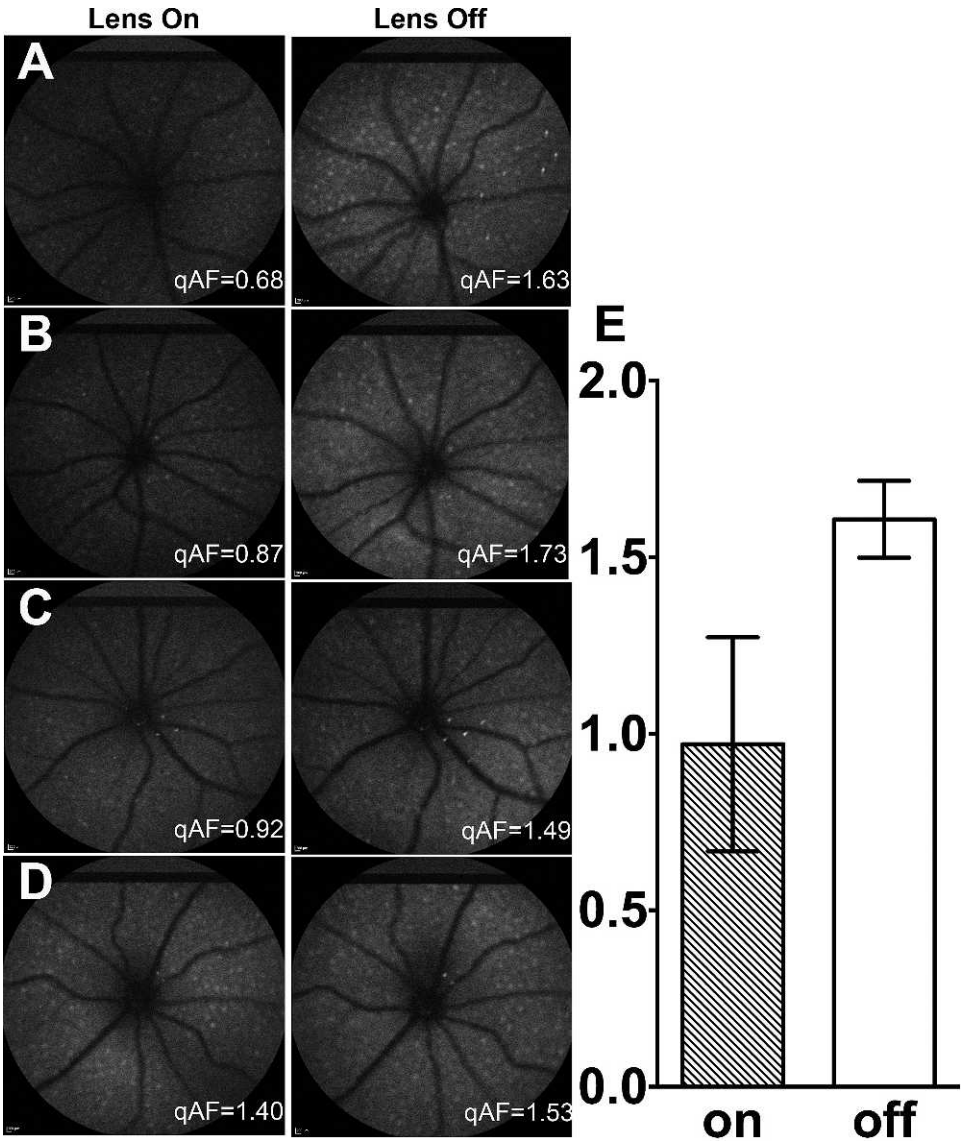


FIGURE 2. Effect of contact lens on qAF values. In 4 mice ([**A**–**D**]; BALB/c mice, age 10 months) a set of 3 images was acquired with contact lens in place (*left column*) and a set without contact lens (*right column*). qAF values for the images shown are indicated in *white*. (**E**) Mean qAF (±SD) of 3 images from each of 4 mice with contact lens on and off.

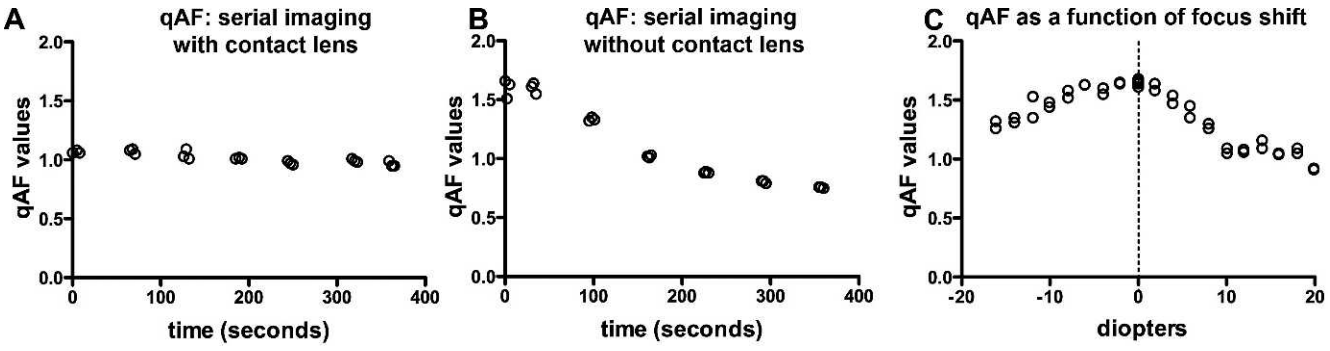


FIGURE 3. qAF with and without a contact lens, and with defocusing. With contact lens (**A**) and no contact lens (**B**), serial images were acquired at 60-second intervals in BALB/c mice (age 10 months). (**C**) qAF values in images acquired at a focus that yielded the highest reflectance in NIR-R mode (0), and with 2 diopter shifts in hyperopic (+) and myopic (–) directions in a *Abca4*$^{-/-}$ mouse (age 10 months). Each *circle* represents the value from one image.

### qAF Repeatability

We tested the intersession repeatability of qAF while imaging 5 *Abca4*$^{-/-}$ mice (age 6 months) without the contact lens. The Bland-Altman coefficient of repeatability (95% confidence interval) was ±18.6% for measurements between first and second sessions, with the mouse and camera being repositioned between sessions. Thus, an image taken in a second session can be expected to differ from the first session by more than 18.6% only 5% of the time. Intersession differences in qAF values were not statistically significant (unpaired *t*-test, $P > 0.05$).

### qAF Values as a Function of Genotype and Age

We measured fundus AF levels in *Abca4*$^{-/-}$, *Abca4*$^{+/-}$, and *Abca4*$^{+/+}$ mice at 2, 4, 8, and 12 months of age (without a contact lens) to calculate qAF values averaged over all segments. Measurements revealed an age-related increase in fundus AF intensities in all genotypes (Fig. 4A). qAF intensities in *Abca4* null mutant mice from 2 to 12 months of age were 1.8- to 2.6-fold greater than in *Abca4*$^{+/+}$ mice ($P < 0.05$). qAF values in heterozygous mice (*Abca4*$^{+/-}$) also were consistently greater than in wild-type mice (*Abca4*$^{+/+}$), but here the average difference was only 15% and did not reach statistical significance ($P > 0.05$).

As a measure of the consistency of the values, the coefficient of variation (CV) (SD/mean × 100) for *Abca4*$^{-/-}$, *Abca4*$^{+/-}$, and *Abca4*$^{+/+}$ mice at 4 months of age was ±29.2%, ±30.5%, and ±26.2%, respectively. Within-session repeatability (Bland-Altman coefficient), determined using values for *Abca4*$^{-/-}$ mice at 6 months of age, was ±23.2%. Differences in qAF between images 1 and 2 in single sessions were not statistically significant (unpaired *t*-test, $P > 0.05$).

Linear regression was used to compare the rates of increase in qAF from 2 to 8 months of age. The slopes (±SE) of the regression lines for *Abca4*$^{+/+}$ (0.09 ± 0.02) and *Abca4*$^{+/-}$ (0.11 ± 0.03) mice differed significantly from *Abca4*$^{-/-}$ (0.19 ± 0.04), but the slopes for *Abca4*$^{+/+}$ and *Abca4*$^{+/-}$ were not significantly different (one-way ANOVA and Tukey's multiple comparison test, 0.05 level of significance).

### HPLC Quantitation of A2E

A2E, a bisretinoid compound of RPE lipofuscin, was quantified by integrating HPLC peak areas and normalizing to a calibration curve. As shown previously,[28,29] A2E levels were increased considerably in *Abca4*$^{-/-}$ mice compared to wild-type (Fig. 4B). Levels of A2E in heterozygous mice were intermediate between *Abca4*$^{-/-}$ and *Abca4*$^{+/+}$ mice. For instance, at 2 and 4 months of age the mean content of A2E in *Abca4*$^{-/-}$ mice was 4- and 2.8-fold greater, respectively, than in *Abca4*$^{+/+}$ mice ($P < 0.05$). Conversely, in *Abca4*$^{+/-}$ mice the difference was 1.5- and 2-fold (*Abca4*$^{+/-}$ versus *Abca4*$^{+/+}$ at 2 and 4 months, respectively; $P < 0.05$ at 4 months).

Linear regression was used to compare the rates of increase in A2E from 2 to 8 months of age. The slopes (±SE) of the regression lines for *Abca4*$^{+/+}$ (0.85 ± 0.18) and *Abca4*$^{+/-}$ (1.23 ± 0.19) mice differed significantly from the linear slope for *Abca4*$^{-/-}$ (2.86 ± 0.65) but the slopes for *Abca4*$^{+/+}$ and *Abca4*$^{+/-}$ were not significantly different (one-way ANOVA and Tukey's multiple comparison test). However, a quadratic regression model better described the increase in A2E with age (quadratic coefficient 0.30 ± 0.06) as attested to by a higher goodness of fit ($R^2 = 0.70$) compared to that for the linear regression ($R^2 = 0.61$). For the *Abca4*$^{-/-}$ mice, the slope of the quadratic was 1.2, 2.4, 3.6, and 4.8 at 2, 4, 6, and 8 months of age, respectively.

In Figure 4C, we plotted average values of qAF as a function of A2E at each age and genotype. Also shown is a line fit by weighted linear regression through the data of all genotypes. Multiple regression analysis of the weighted data showed no significant association with $A2E^2$, age, and genotype, and no significant genotype–age interaction. The slope of the line was 0.10 ± 0.01 qAF-units per pmol/eye (±SE, $P < 0.0001$) and the intercept was 0.7 ± 0.1 qAF units ($P > 0.0001$). These findings indicated that qAF and A2E are not proportional to each other.

For all 3 genotypes, A2E accumulates with age more rapidly than qAF. For qAF and A2E, and for all 3 genotypes, we calculated the ratio of the measure at age 8 months to the measure at age 2 months, as a simple indicator of relative accumulation. For A2E and qAF, respectively, these ratios are 3.0 ± 0.6 and 1.7 ± 0.1 in *Abca4*$^{+/+}$ mice, 3.1 ± 0.7 and 1.8 ±

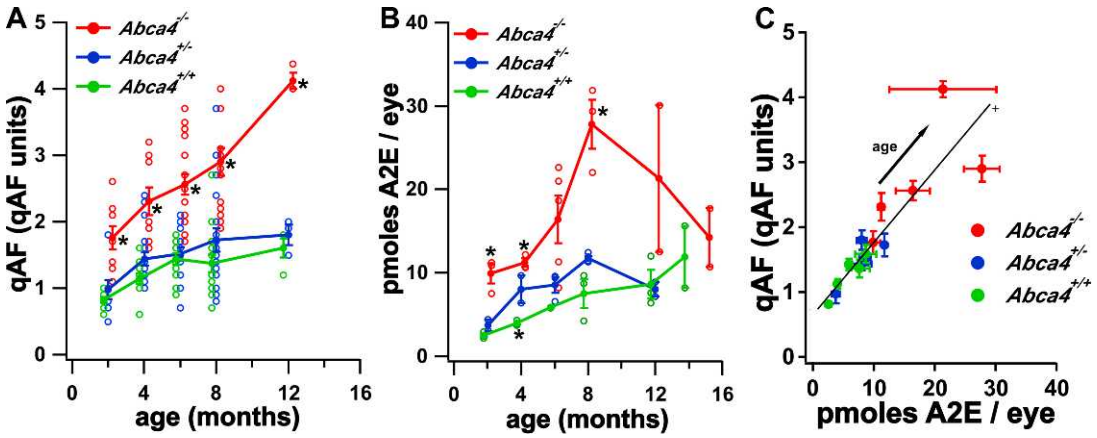


**Figure 4.** Measurement of fundus AF and A2E in mice. (**A**) qAF as a function of genotype and age in mice. Values are normalized intensities and the average of the 8 segments presented in Figure 1. Means ± SEM are based on 9 to 18 mice at ages 2 to 8 months and 3 to 4 mice at 12 months. *$P <$ 0.05, one-way ANOVA and Tukey's multiple comparison test. (**B**) Quantitation of the bisretinoid A2E in *Abca4*$^{-/-}$, *Abca4*$^{+/-}$, and *Abca4*$^{+/+}$ mice. Measurement by reverse phase HPLC. Values are mean ± SEM; 4 to 8 eyes per sample, 2 to 5 independent samples/mean. *Error bars* are not visible if smaller than the symbol. Statistical analysis by one-way ANOVA and Tukey's multiple comparison test; $P < 0.05$ for *Abca4*$^{-/-}$ versus *Abca4*$^{+/+}$ at 2, 4, 8 months; *Abca4*$^{+/-}$ versus *Abca4*$^{+/+}$ at 4 months. (**C**) qAF plotted as a function of A2E for *Abca4*$^{-/-}$, *Abca4*$^{+/-}$, and *Abca4*$^{+/+}$ mice. Values are the mean ± SEM for each age (2–12 months). The *solid line* is the weighted linear fit through the data from the 3 genotypes. The weights were calculated as the inverse of the square root of ($SE_{A2E}^2 - SE_{qAF}^2$).

0.2 for *Abca4*$^{+/-}$ mice, and 2.8 ± 1.6 and 1.6 ± 0.2 in *Abca4*$^{-/-}$ mice.

### ONL Thickness

We evaluated photoreceptor cell viability in *Abca4*$^{-/-}$, *Abca4*$^{+/-}$, and *Abca4*$^{+/+}$ mice by measuring ONL thickness. ONL width was plotted in 200 μm intervals superior and inferior to the ONH in the vertical plane. Results are presented in Figure 5. ONL thickness at 4 months of age was not statistically different among the 3 genotypes (one-way ANOVA, $P > 0.05$). However, at 8 months of age, ONL thinning was observed in *Abca4*$^{-/-}$ and *Abca4*$^{+/-}$ mice. For instance in *Abca4*$^{-/-}$ mice, at 0.4 mm superior and inferior to ONH there was a 19% and 24% reduction, respectively, in ONL width compared to *Abca4*$^{+/+}$ mice ($P < 0.05$). The thinning in *Abca4*$^{-/-}$ mice was accentuated further at age 12 months. ONL thickness also was reduced in *Abca4*$^{+/-}$ mice at 8 months of age, and at 12 months of age ONL thinning in the heterozygous mice had progressed such that thickness was significantly different from *Abca4*$^{+/+}$ mice at 13 months of age (0.2–2.0 mm superiorly and inferiorly, $P < 0.05$). Wild-type mice did not exhibit ONL thinning even at age 15 months.

## Discussion

Fundus AF originates principally from the lipofuscin that accumulates in RPE cells. The bisretinoid compounds in RPE lipofuscin have the spectral characteristics consistent with fundus AF, and these fluorophores form in photoreceptor outer segments as a consequence of inadvertent reactions of vitamin A-aldehyde.[30] A2E is a well-known bisretinoid of RPE lipofuscin,[31,32] but other bisretinoids have been characterized.[33] By qAF analysis and by HPLC measurement of A2E in mice, we replicated previous findings demonstrating that RPE lipofuscin increases with age in humans[34–36] and mice.[29,37] In our current study, qAF increased with age from 2 to 12 months in *Abca4*$^{+/+}$, *Abca4*$^{+/-}$, and *Abca4*$^{-/-}$ mice. The slope of the regression line describing the qAF increase with age in *Abca4*$^{-/-}$ mice was significantly greater than for *Abca4*$^{+/-}$ and *Abca4*$^{+/+}$ mice; this finding indicated a more rapid rate of qAF increase in *Abca4*$^{-/-}$ mice. The regression line reflecting the change in A2E levels with age also was steeper in the case of *Abca4*$^{-/-}$. The increase in A2E observed in *Abca4*$^{+/-}$ mice relative to *Abca4*$^{+/+}$ replicated a previous report.[38]

By plotting qAF as a function of A2E (Fig. 4C) we found that the data fit a linear model but the significant positive intercept (0.7 qAF units) along the qAF axis indicated that proportionality between the two measures could not be demonstrated. However, if all qAF measurements were reduced by 0.7, proportionality would be realized. One interpretation of the positive intercept in the linear relationship between qAF and A2E is that fluorophore(s) that do not accumulate contribute to qAF measurements in addition to A2E (and other bisretinoids[33] that accumulate at the same rate). This interpretation assumes that these other fluorophore(s) provide a constant contribution to qAF at all ages and genotypes. The amount of the additional fluorophore(s) could remain constant if these were bisretinoid precursors or were processed otherwise (e.g., oxidation, Schiff base hydrolysis). One cannot exclude contributions to qAF from retinal tissues and from the superficial choroid, since the depth of focus of the Spectralis is approximately 300 μm.

Comparison of the increases in qAF and A2E with age revealed that A2E levels increased faster than the qAF levels for all genotypes. This is explained partially by our model, since removing the contribution of the other fluorophore from all qAF data essentially would increase the ratios of qAF at age 8 months to qAF at age 2 months, and bring these ratios closer to those obtained for A2E. Thus, for *Abca4*$^{+/+}$ mice the ratio would increase from 1.7 ± 0.1 to 5.4 ± 0.1 (compared to 3.0 ± 0.6 for A2E), for *Abca4*$^{+/-}$ mice the ratio would increase from 1.8 ± 0.2 to 3.6 ± 0.2 (compared to 3.1 ± 0.7 for A2E), and for *Abca4*$^{-/-}$ mice the ratio would increase from 1.6 ± 0.2 to 2.1 ± 0.2 (compared to 2.8 ± 1.6 for A2E).

The discrepancy in A2E and qAF in terms of the linear versus quadratic time course, may be the result of self-absorption in the RPE during the in vivo measurement of qAF. Indeed, the lipofuscin-containing residual bodies are distributed at various levels in the cell and high absorption by lipofuscin in the apical part of the cell will reduce the contribution of the more deeply positioned lipofuscin. Thus, the qAF signal could be attenuated in older *Abca4*$^{-/-}$ mice wherein the quantity of lipofuscin is the highest. Since we used albino mice for this study, absorbance of fluorescence signal by melanin would not be a factor.

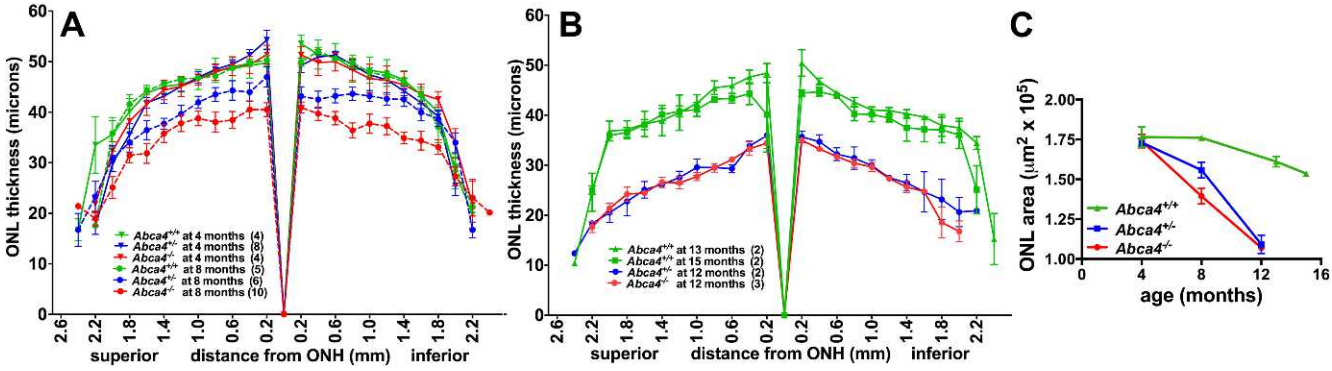


Figure 5. Quantification of ONL thickness in *Abca4*$^{-/-}$, *Abca4*$^{+/-}$, and *Abca4*$^{+/+}$ mice at ages 4 and 8 months (**A**), and ages 12 to 15 months (**B**). Measurements are plotted as a function of distance from the ONH in the inferior and superior hemispheres. Numbers of mice are presented in parentheses. Mean ± SEM. Significant differences were determined by one-way ANOVA and Tukey's multiple comparison test, $P < 0.05$: *Abca4*$^{-/-}$ age 8 vs. 4 months, 0.2 to 1.8 mm superiorly, and 0.2 to 1.8 mm inferiorly; *Abca4*$^{-/-}$ versus *Abca4*$^{+/+}$ at age 8 months, 0.2 to 2.0 mm superiorly, and 0.2 to 1.6 mm inferiorly; *Abca4*$^{+/-}$ versus *Abca4*$^{+/+}$ at age 8 months, 1.4 mm superiorly, and 0.2 to 0.6 mm inferiorly; *Abca4*$^{+/-}$ (12 months) versus *Abca4*$^{+/+}$ (13 months) at age 8 months, 0.2 to 2.0 mm superiorly and inferiorly. (**C**) Progression of photoreceptor cell loss plotted as decreasing ONL area. The latter was calculated by summing ONL thicknesses (2.0 superiorly to 1.8 inferiorly) and multiplying by the measurement interval of 200 μm. Mean ± SEM.

In addition to formation of lipofuscin, a factor to take into consideration is removal of lipofuscin. Such a process might be invoked to explain the declining rates of increase in qAF and A2E (Fig. 4). No evidence exists for enzyme-mediated degradation of RPE bisretinoids. However, photodegradation of bisretinoid secondary to photooxidation is known to occur. Photooxidation manifested as fluorescence bleaching (i.e., a decline in fluorescence emission) has been observed within RPE by noninvasive in vivo fundus AF imaging[39] and in culture models.[40] Thus, final qAF is the product of the ratio of fluorophore synthesis in photoreceptor cells versus fluorophore photobleaching in RPE. Moreover, since the products of bisretinoid photodegradation are damaging, it is possible that the lipofuscin lost by photooxidation-associated photodegradation is more significant than the lipofuscin remaining in the cells. It is tempting to consider the possibility that the tendency for photooxidation of bisretinoid varies with bisretinoid concentration, but at this time we have no evidence of this.

The decline in HPLC measurable A2E observed after 8 months of age in *Abca4*$^{-/-}$ mice corresponded to the photoreceptor cell loss that was detected as a reduction in ONL thickness at 8 months of age. The thinning of ONL had progressed at 12 months of age. The latter result replicates our previous findings[25] and that of others.[41] We also observed a less pronounced thinning of ONL in *Abca4*$^{+/-}$ mice. We did not observe an age-related thinning of ONL in *Abca4*$^{+/+}$ mice even at 15 months of age. Consistent with this, most studies of wild-type mice have reported age-associated photoreceptor cell death only after 17 to 24 months of age.[42–44] Whether the loss of photoreceptor cells occurs consequent to RPE cell degeneration is not yet known. Nevertheless, these findings indicated a relationship between RPE lipofuscin accumulation and photoreceptor cell death. Specifically, the increase in A2E levels and the decrease in ONL thickness (8 months of age) in the *Abca4*$^{+/-}$ mice were less pronounced than in *Abca4*$^{-/-}$ mice. It also is notable that A2E levels and qAF in *Abca4*$^{+/-}$ mice were more similar to wild-type than to *Abca4*$^{-/-}$ mice. This finding could indicate that with one-half of the gene dosage, Abca4 protein expression is sufficient to prevent substantially increased bisretinoid formation. What was striking to us was that despite the continued loss of photoreceptor cells between 8 and 12 months of age, and the decline in A2E levels, qAF values continued to be elevated. This is an observation deserving further investigation. We previously have provided evidence that increased fundus AF can accompany photoreceptor cell dysfunctioning and degeneration.[30,45] Thus, perhaps the pronounced fundus AF after 8 months of age reflects the photoreceptor cell degeneration documented by ONL thinning. The identities of the bisretinoids accounting for this continued increase in qAF are not known, but they are unlikely to include A2E as the latter fluorophore exhibited decreased levels after 8 months of age. Other bisretinoids detected by fundus AF could include A2PE the precursor of A2E located in photoreceptor outer segments.[46] Whether this scenario provides an explanation for our current findings is not yet known.

Charbel Issa et al. recently reported gray level analysis of fundus AF images using a wide-field 55° lens, the use of a constant detector sensitivity, and the acquisition of non-normalized images.[14] Image gray levels were determined along a horizontal profile through the disc with application of a Gaussian blur to reduce image noise and subtraction of zero-gray level. Correction for variable laser power was not performed. The detection pupil used was the pupil of the mouse, thereby requiring a correction for pupil diameter. They observed a 2-fold difference in autofluorescence intensity between pigmented *Abca4*$^{-/-}$ mice versus wild-type at 6 months of age; the fold-difference in our study was 2.7 in albino *Abca4*$^{-/-}$ mice at 6 months of age.

The intersession coefficient of repeatability calculated in our work (±18.6%, in the absence of a contact lens) was similar to that reported by Charbel Issa et al., (±22%, with contact lens)[14] in mice, but was less satisfactory than that obtained for human subjects (±6%–11).[24] One difference between human subjects and mice is that determining optimal focus in mice can be more difficult. Thus, in our hands between-session differences in the chosen focus setting was found to be greater (2–3 D) than with fundus AF imaging in humans (0.20–0.27 D). At the same time, however, we found that there is a considerably smaller qAF change per D defocusing in mice compared to humans. Consistent with this, Charbel Issa et al. reported that defocusing within a range of 4 D did not result in appreciable changes in fluorescence intensity values.[14] They observed that after focusing in the NIR reflectance mode, a +8 to +10 D dioptric correction was required to focus in the same retinal plane for 488 nm imaging. We used a smaller detection pupil (0.98 mm, compared to the full pupil diameter used by Charbel Issa et al.[14]) and did not observe a similar dioptric shift. It is likely that the use of a smaller aperture increases the depth of focus, and reduces spherical and chromatic aberrations in the mouse eye. Charbel Issa et al. also emphasized the utility of a contact lens in retarding cataract formation and in providing a standardized curvature to the eye.[14] In addition, we observed that with the contact lens, the point of optimal focus was somewhat more hyperopic than without the contact lens. However, we preferred not to use the contact lens during imaging because variability without the lens was lower than in the presence of the contact lens. Also, attenuation of the AF signal by the contact lens was not constant, perhaps because of varying amounts of gel underneath the lens or due to differences in alignment of the lens.

We concluded that in preclinical studies using mouse models, a standardized approach to fundus AF imaging combined with an internal fluorescent reference enables reliable measurement of normal and disease-related fundus AF in mouse models. The advantages of this approach to RPE lipofuscin quantitation are that repeated in vivo measurements can be performed efficiently and fewer mice are required.

## Acknowledgments

The authors thank Joerg Fischer, Heidelberg Engineering, Germany for his expertise.

Supported by National Institutes of Health Grants P30EY019007, R24EY019861, EY12951, Foundation Fighting Blindness, and by a grant from Research to Prevent Blindness to the Department of Ophthalmology, Columbia University.

Disclosure: **J.R. Sparrow**, None; **A. Blonska**, None; **E. Flynn**, None; **T. Duncker**, None; **J.P. Greenberg**, None; **R. Secondi**, None; **K. Ueda**, None; **F.C. Delori**, None

## References

1. Delori FC. RPE lipofuscin in ageing and age-related macular degeneration. In: Coscas G, Piccolino FC, eds. *Retinal Pigment Epithelium and Macular Disease (Documenta Ophthalmologica)*. Dordrecht, The Netherlands: Kluwer Academic Publishers; 1995:37–45.
2. Delori FC, Goger DG, Dorey CK. Age-related accumulation and spatial distribution of lipofuscin in RPE of normal subjects. *Invest Ophthalmol Vis Sci*. 2001;42:1855–1866.

3. Delori FC, Staurenghi G, Arend O, Dorey CK, Goger DG, Weiter JJ. In vivo measurement of lipofuscin in Stargardt's disease–Fundus flavimaculatus. *Invest Ophthalmol Vis Sci*. 1995;36:2327–2331.
4. Delori FC, Dorey CK, Staurenghi G, Arend O, Goger DG, Weiter JJ. In vivo fluorescence of the ocular fundus exhibits retinal pigment epithelium lipofuscin characteristics. *Invest Ophthalmol Vis Sci*. 1995;36:718–729.
5. Allikmets R, Singh N, Sun H, et al. A photoreceptor cell-specific ATP-binding transporter gene (ABCR) is mutated in recessive Stargardt macular dystrophy. *Nat Genet*. 1997;15:236–246.
6. von Ruckmann A, Fitzke FW, Bird AC. Distribution of fundus autofluorescence with a scanning laser ophthalmoscope. *Br J Ophthalmol*. 1995;79:407–412.
7. Holz FG, Bellmann C, Margaritidis M, Schutt F, Otto TP, Volcker HE. Patterns of increased in vivo fundus autofluorescence in the junctional zone of geographic atrophy of the retinal pigment epithelium associated with age-related macular degeneration. *Graefe's Arch Clin Exp Ophthalmol*. 1999;237:145–152.
8. Lois N, Owens SL, Coco R, Hopkins J, Fitzke FW, Bird AC. Fundus autofluorescence in patients with age-related macular degeneration and high risk of visual loss. *Am J Ophthalmol*. 2002;133:341–349.
9. Robson AG, Saihan Z, Jenkins SA, et al. Functional characterisation and serial imaging of abnormal fundus autofluorescence in patients with retinitis pigmentosa and normal visual acuity. *Br J Ophthalmol*. 2006;90:472–479.
10. Robson AG, Lenassi E, Saihan Z, et al. Comparison of fundus autofluorescence with photopic and scotopic fine matrix mapping in patients with retinitis pigmentosa: 4- to 8-year follow-up. *Invest Ophthalmol Vis Sci*. 2012;53:6187–6195.
11. Robson AG, Michaelides M, Luong VA, et al. Functional correlates of fundus autofluorescence abnormalities in patients with RPGR or RIMS1 mutations causing cone or cone rod dystrophy. *Br J Ophthalmol*. 2008;92:95–102.
12. Cideciyan AV, Aleman TS, Swider M, et al. Mutations in ABCA4 result in accumulation of lipofuscin before slowing of the retinoid cycle: a reappraisal of the human disease sequence. *Hum Mol Genet*. 2004;13:525–534.
13. Lois N, Halfyard A, Bird AC, Fitzke FW. Quantitative evaluation of fundus autofluorescence imaged 'in vivo' in eyes with retinal disease. *Br J Ophthalmol*. 2000;84:741–745.
14. Charbel Issa P, Singh MS, Lipinski DM, et al. Optimization of in vivo confocal autofluorescence imaging of the ocular fundus in mice and its application to models of human retinal degeneration. *Invest Ophthalmol Vis Sci*. 2012;53:1066–1075.
15. Secondi R, Kong J, Blonska AM, Staurenghi G, Sparrow JR. Fundus autofluorescence findings in a mouse model of retinal detachment. *Invest Ophthalmol Vis Sci*. 2012;53:5190–5197.
16. Huber G, Beck SC, Grimm C, et al. Spectral domain optical coherence tomography in mouse models of retinal degeneration. *Invest Ophthalmol Vis Sci*. 2009;50:5888–5895.
17. Allocca M, Doria M, Petrillo M, et al. Serotype-dependent packaging of large genes in adeno-associated viral vectors results in effective gene delivery in mice. *J Clin Invest*. 2008;118:1955–1964.
18. Kong J, Kim SR, Binley K, et al. Correction of the disease phenotype in the mouse model of Stargardt disease by lentiviral gene therapy. *Gene Ther*. 2008;15:1311–1320.
19. Radu RA, Mata NL, Nusinowitz S, Liu X, Sieving PA, Travis GH. Treatment with isotretinoin inhibits lipofuscin and A2E accumulation in a mouse model of recessive Stargardt's macular degeneration. *Proc Natl Acad Sci U S A*. 2003;100:4742–4747.
20. Radu RA, Han Y, Bui TV, et al. Reductions in serum vitamin A arrest accumulation of toxic retinal fluorophores: a potential therapy for treatment of lipofuscin-based retinal diseases. *Invest Ophthalmol Vis Sci*. 2005;46:4393–4401.
21. Maeda A, Maeda T, Golczak M, et al. Effects of potent inhibitors of the retinoid cycle on visual function and photoreceptor protection from light damage in mice. *Mol Pharmacol*. 2006;70:1220–1229.
22. Maiti P, Kong J, Kim SR, Sparrow JR, Allikmets R, Rando RR. Small molecule RPE65 antagonists limit the visual cycle and prevent lipofuscin formation. *Biochem*. 2006;45:852–860.
23. Maeda A, Golczak M, Chen Y, et al. Primary amines protect against retinal degeneration in mouse models of retinopathies. *Nat Chem Biol*. 2011;8:170–178.
24. Delori FC, Greenberg JP, Woods RL, et al. Quantitative measurements of autofluorescence with the scanning laser ophthalmoscope. *Invest Ophthalmol Vis Sci*. 2011;52:9379–9390.
25. Wu L, Nagasaki T, Sparrow JR. Photoreceptor cell degeneration in *Abcr*$^{-/-}$ mice. *Adv Exp Med Biol*. 2010;664:533–539.
26. Bermudez MA, Vicente AF, Romero MC, Arcos MD, Abalo JM, Gonzalez F. Time course of cold cataract development in anesthetized mice. *Curr Eye Res*. 2011;36:278–284.
27. Sparrow JR, Kim SR, Wu Y. Experimental approaches to the study of A2E, a bisretinoid lipofuscin chromophore of retinal pigment epithelium. *Method Mol Biol*. 2010;652:315–327.
28. Kim SR, Fishkin N, Kong J, Nakanishi K, Allikmets R, Sparrow JR. The Rpe65 Leu450Met variant is associated with reduced levels of the RPE lipofuscin fluorophores A2E and iso-A2E. *Proc Natl Acad Sci U S A*. 2004;101:11668–11672.
29. Mata NL, Weng J, Travis GH. Biosynthesis of a major lipofuscin fluorophore in mice and humans with ABCR-mediated retinal and macular degeneration. *Proc Natl Acad Sci U S A*. 2000;97:7154–7159.
30. Sparrow JR, Yoon K, Wu Y, Yamamoto K. Interpretations of fundus autofluorescence from studies of the bisretinoids of retina. *Invest Ophthalmol Vis Sci*. 2010;51:4351–4357.
31. Eldred GE, Lasky MR. Retinal age pigments generated by self-assembling lysosomotropic detergents. *Nature*. 1993;361:724–726.
32. Parish CA, Hashimoto M, Nakanishi K, Dillon J, Sparrow JR. Isolation and one-step preparation of A2E and iso-A2E, fluorophores from human retinal pigment epithelium. *Proc Natl Acad Sci U S A*. 1998;95:14609–14613.
33. Sparrow JR, Gregory-Roberts E, Yamamoto K, et al. The bisretinoids of retinal pigment epithelium. *Prog Retin Eye Res*. 2012;31:121–135.
34. Wing GL, Blanchard GC, Weiter JJ. The topography and age relationship of lipofuscin concentration in the retinal pigment epithelium. *Invest Ophthalmol Vis Sci*. 1978;17:601–607.
35. Feeney-Burns L, Hilderbrand ES, Eldridge S. Aging human RPE: morphometric analysis of macular, equatorial, and peripheral cells. *Invest Ophthalmol Vis Sci*. 1984;25:195–200.
36. Weiter JJ, Delori FC, Wing GL, Fitch KA. Retinal pigment epithelial lipofuscin and melanin and choroidal melanin in human eyes. *Invest Ophthalmol Vis Sci*. 1986;27:145–151.
37. Kim SR, He J, Yanase E, et al. Characterization of dihydro-A2PE: an Intermediate in the A2E biosynthetic pathway. *Biochem*. 2007;46:10122–10129.
38. Mata NL, Tzekov RT, Liu X, Weng J, Birch DG, Travis GH. Delayed dark adaptation and lipofuscin accumulation in abcr+/– mice: implications for involvement of *ABCR* in age-related macular degeneration. *Invest Ophthalmol Vis Sci*. 2001;42:1685–1690.
39. Hunter JJ, Morgan JI, Merigan WH, Sliney DH, Sparrow JR, Williams DR. The susceptibility of the retina to photochemical damage from visible light. *Prog Retin Eye Res*. 2012;31:28–42.


Investigative Ophthalmology & Visual Science

40. Yamamoto K, Zhou J, Hunter JJ, Williams DR, Sparrow JR. Toward an understanding of bisretinoid autofluorescence bleaching and recovery. *Invest Ophthalmol Vis Sci*. 2012;53:3536–3544.
41. Radu RA, Yuan Q, Hu J, et al. Accelerated accumulation of lipofuscin pigments in the RPE of a mouse model for ABCA4-mediated retinal dystrophies following Vitamin A supplementation. *Invest Ophthalmol Vis Sci*. 2008;49:3821–3829.
42. Chang B. Age-related eye disease. In: Chalupa LM, Williams RW, eds. *Eye, Retina and Visual System of the Mouse*. Cambridge, MA: The MIT Press; 2008:581–590.
43. Gresh J, Goletz PW, Crouch RK, Rohrer B. Structure–function analysis of rods and cones in juvenile, adult, and aged C57BL/6 and Balb/c mice. *Vis Neurosc*. 2003;20:211–220.
44. Bravo-Nuevo A, Walsh N, Stone J. Photoreceptor degeneration and loss of retinal function in the C57BL/6-C2J mouse. *Invest Ophthalmol Vis Sci*. 2004;45:2005–2012.
45. Gelman R, Chen R, Blonska A, Barile G, Sparrow JR. Fundus autofluorescence imaging in a patient with rapidly developing scotoma. *Retin Cases Brief Rep*. 2012;6:345–348.
46. Ben-Shabat S, Parish CA, Vollmer HR, et al. Biosynthetic studies of A2E, a major fluorophore of RPE lipofuscin. *J Biol Chem*. 2002;277:7183–7190.

Investigative Ophthalmology & Visual Science